Shock Tube Measurements of the Equation of State of Argon[1]

D. F. Davidson,[2,3] R. Bates,[2,4] E. L. Petersen,[2] and R. K. Hanson [2]

---

[1] Paper presented at the Thirteenth Symposium on Thermophysical Properties, June 22-27, 1997, Boulder, Colorado, U.S.A.

[2] High Temperature Gasdynamics Laboratory, Thermosciences Division, Department of Mechanical Engineering, Stanford University, Stanford, California 94305, U.S.A.

[3] To whom correspondence should be addressed.

[4] United States Air force Palace Knight, Phillips Laboratory, Edwards Air Force Base, California, USA.

ABSTRACT

We have investigated the equation of state of argon at elevated temperatures and pressures using a new shock tube method. Temperatures in the range 1280 to 1830 K, and pressures from 60 to 500 atm were generated behind reflected shock waves in test gas mixtures of argon with trace amounts of CO and H_2 added. Density was determined from reflected shock pressure and incident shock speed measurements using the shock-jump relations. Temperature was determined from the modeling of the 4.7μ infrared emission of the fundamental vibrational band of thermally-equilibrated CO. The experimentally-determined argon P-ρ-T data points are in good agreement with the static-cell data of LeCocq (1960) and an extrapolation of the equation of state of Stewart-Jacobsen (1989).

KEY WORDS: argon, equation of state, experimental measurement, high pressure, high temperature, infrared emission, P-ρ-T data, shock tube

1. INTRODUCTION

There has been renewed interest in the combustion community in high-pressure, high-temperature (HP/HT) chemistry and the importance of real gas equations of state in these systems. This has been motivated by the need to better understand and model processes in devices such as diesel engines, ram accelerators, rockets, and super-critical incinerators [1-3]. Accurate calculations of these processes are hindered by the lack of HP/HT equation of state (EOS) data for most combustion species.

Argon is an important buffer gas used in HP/HT combustion-related shock tube experiments. Its properties dominate the thermodynamics of the experiments in which it is the largest constituent, and yet experimental validation studies of the argon EOS at combustion temperatures are rare. Two recent reviews of the argon EOS [4,5] have indicated that only one reliable investigation, a static cell study by LeCocq [6], extends the range of argon P-ρ-T measurements above 673 K. Fig. 1 shows the current state of high temperature P-ρ-T measurements of argon. Clearly, there is a need to confirm the argon P-ρ-T behavior at HP/HT, which at present is predicted only by extrapolating current EOS from lower temperature regimes. To this end, we performed a series of experiments to measure the argon EOS at high temperatures and pressures using a novel shock tube method, and report the results here.

2. EQUATION OF STATE MEASUREMENTS

The method used to measure EOS state variables in this study is based on two properties of shock wave flow. A schematic representation of this flow is shown in Fig. 2. First, the test gas density found in the reflected region of shock wave experiments is

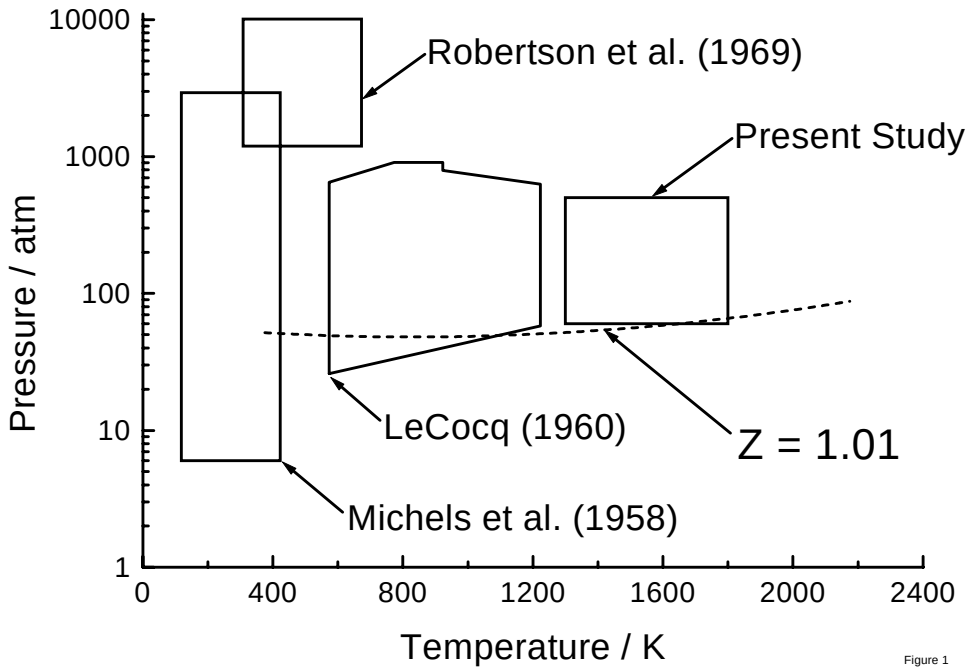

Fig. 1. Selected Argon P-ρ-T Measurements. A large selection of low temperature work, particularly near the critical point, is not included in this figure.

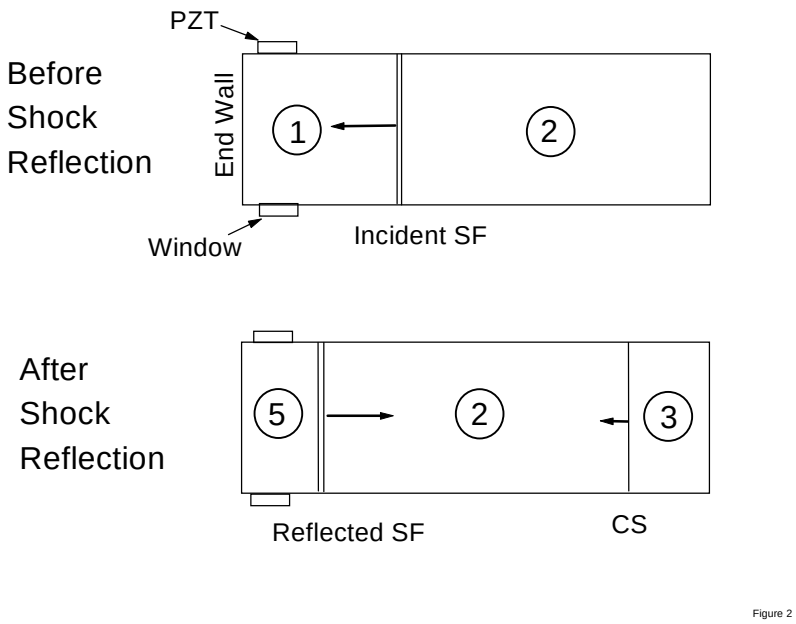

Fig. 2. Schematic of Shock Tube Flow. Upper panel, incident shock; lower panel, reflected shock. Region 1, initial conditions; region 2, post-incident shock; region 5, post-reflected shock. SF, shock front; CS, contact surface separating the argon test gas from the driver helium gas of region 3.

determined by the incident shock speed, V_S, and post-incident shock conditions, and a single measurable state variable of the reflected shock region, the pressure P_5. Thus the density in the reflected shock regime is decoupled from the reflected shock temperature and can be determined separately from it. Second, the reflected shock temperature, T_5, because of real gas effects, has a lower value than that predicted from calculations using the ideal gas EOS. This lower temperature has a very marked influence on infrared emission from the test gas in the reflected shock region, and variation of this emission as a function of temperature can be predicted accurately, if the density is known.

2.1 Shock Tube Facility

Elevated test gas temperatures and pressures were produced by shock heating and compression in a new helium-driven, high-pressure, high-purity shock tube in our laboratory. Details of its construction can be found in Davidson and Hanson [9]. Shock velocities, V_S, are determined from incident shock arrival times measured over six 300 mm intervals along the driven body of the shock tube. Uncertainty in the time interval measurement is ±0.3 μs, and incident shock attenuations are typically 2-3%/m at the endwall. Reflected shock pressure, P_5, measurements have been made with a thermally-protected Kistler piezoelectric transducer (PZT) located in the shock tube side wall 20 mm from the end wall. Test gas were mixed manometrically using ultra-high purity gases in a separate aluminum mixing vessel. Typical mixtures were as follows: 1500 ppm CO, 8500 ppm H_2, balance argon (used in the 60 atm calibration and 165 atm data); 750 ppm CO, 4250 ppm H_2, balance argon (used in the 300 atm data); and 500 ppm CO, 2850 ppm H_2,

balance argon (used in the 500 atm data). Hydrogen was added to the mixture to reduce the vibrational relaxation times of CO.

2.2 Real Gas Shock Equation Solver

We calculated the incident- and reflected-shock state variables using two recently available computer codes for the calculation of real gas properties: REAL GAS CHEMKIN [7] and ALLPROPS [10]. We have implemented these two codes as subroutines in a one-dimensional shock equation solver based on standard shock wave theory. The technical details of this solver have been published elsewhere [9].

We note in particular, for the shock conditions described here, that the reflected shock pressures P_5, calculated using the Stewart-Jacobsen real-gas EOS, are within 1% of the ideal calculations everywhere except at the lowest temperature and highest pressure (i.e. 1200 K, 500 atm). Real gas corrections to the ideal reflected shock temperatures, T_5, are approximately -0.085 K atm^{-1} for argon, and the real gas densities, ρ_5, are typically between 5 and 10% less than the ideal values [9].

2.3 Density Determination

The fundamental shock relations can be manipulated to give a simple expression for the reflected shock density ρ_5, as a function of incident shock parameters (ρ_2, P_2, and u_1, u_2, the incoming and outgoing gas speeds in the incident shock-fixed coordinate system) and a single reflected shock property, the pressure P_5 [9].

$$1/\rho_5 = 1/\rho_2 - (u_1 - u_2)^2/(P_5 - P_2) \qquad (1)$$

We assume here that the EOS for argon is near-ideal and well-established in the initial (296 K, up to 10 atm) and incident shock (800 K, up to 100 atm) conditions. In these two

regions, the Stewart-Jacobsen EOS was used in the solution of the shock equations. The incident shock parameters, u_2, and P_2, can be calculated from T_1, P_1, and $V_S = u_1$ using the shock equation solver. P_5 can determined either by assuming an EOS and solving the reflected shock conditions with that EOS, or by actual measurement using a PZT. Actual measurement is clearly preferred, but because the difference between the real gas and the ideal gas calculated reflected shock pressures is usually within 1%, and this difference is only weakly a function of the EOS (occurring as a correction which is second-order in density), both methods give comparable uncertainties. The ±0.5% combined systematic calibration uncertainty and random scatter in the P_5 measurement (or the equivalent uncertainty derived from the assumed EOS) contributes ±0.75% uncertainty to ρ_5; the ±0.1% uncertainty in V_S contributes ±0.5%. The total uncertainty in the determination of ρ_5 is approximately ±0.9%. All data were normalized to 165, 300 or 500 atm.

2.3 Temperature Determination

The reflected shock temperature, T_5, is determined from IR emission measurements collected from the end section of the shock tube using a simple optical collection system incorporating an LN_2-cooled InSb detector. Access through the shock tube wall is via a 6 mm dia sapphire window located 20 mm from the end wall. A spectral filter with a transmission interval 4.18 to 4.74 mm is employed to limit collection of radiation to the R-branch of the CO fundamental band. A small correction (~1%) for black-body emission radiated and reflected from the opposite shock tube wall must be made. An example data record is given in Fig. 3. The emission at time zero is determined by extrapolation of the data obtained in the interval from 100 to 300 μs.

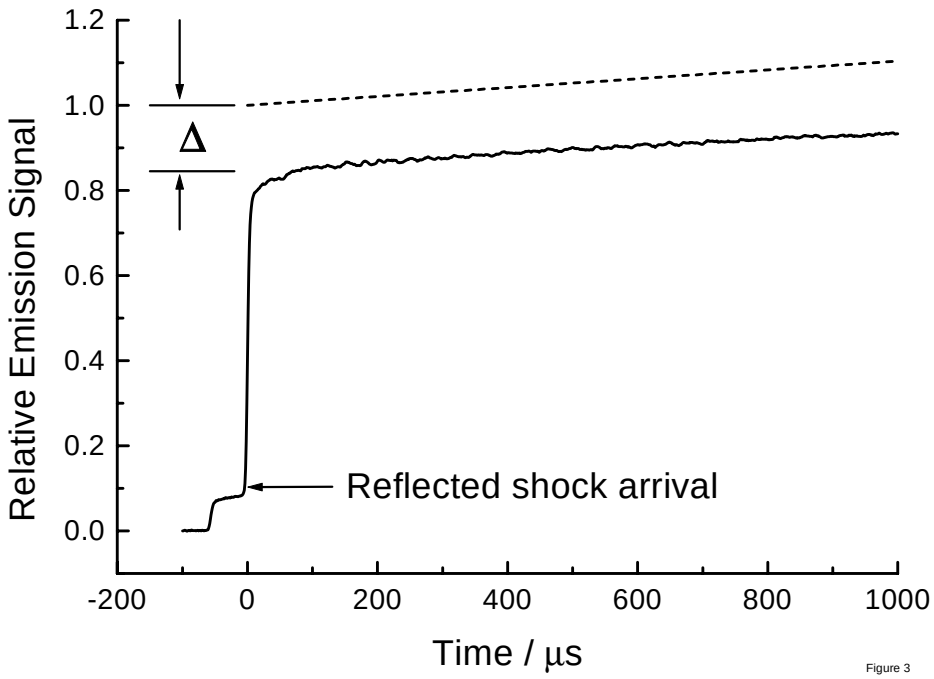

Fig. 3. IR Emission Data at 4.7μ. Reflected shock conditions: 1660 K, 450 atm; mixture: 820 ppm CO/3230 ppm H_2/argon. Δ is the decrement in the emission from real gas effects; dashed line, emission predicted from ideal gas shock calculations; solid line, measured emission.

The IR emission signal of the vibrationally-equilibrated CO population is a function of the total density and CO mass fraction, $\rho_5 X_{CO}$, an optical collection factor F_C, a correction for self-absorption, $F_{SA,}$ and the CO vibrational temperature, θ_v,

$$I_{signal} = F_C F_{SA} \rho_5 X_{CO} / (\exp(\theta_v / T_5) - 1). \quad (2)$$

T_5 can be derived by inverting this equation. The important self-absorption correction has the form $F_{SA} = \exp(-.C_1 \rho_5 X_{CO})$ and has values typically of 0.9. C_1 can be determined by experiment and modeling the CO emission and absorption spectra. The IR spectral constants and line broadening parameters can be found in several works by Vargese and Hanson [11] and others. The optical collection factor, F_C, is determined from the 60 atm calibration shocks where the reflected shock conditions are near-ideal and relatively insensitive to the EOS. The ±0.5% uncertainty in the P_5 measurement contributes ±0.35% uncertainty to T_5, the ±0.1% scatter in V_S contributes 0.2%, and the ±2% scatter in F_C contributes ±0.85%; the total uncertainty in T_5 is approximately ±0.95%.

3. EXPERIMENTAL RESULTS

Argon EOS data collected at pressures near 165, 300 and 500 atm are shown in Fig. 4. Shown also are least-squares fits to the data, the extrapolation of the the Stewart-Jacobsen formulation of the EOS [4], and the experimental results of LeCocq [6]. The data in this figure uses calculated reflected shock pressures derived using the Peng-Robinson EOS [1]. For each nominal pressure range, the data was fit to a temperature-independent second virial coefficient approximation (B(T) = B) of the EOS

$$Z - 1 = B \; P / R T. \quad (3)$$

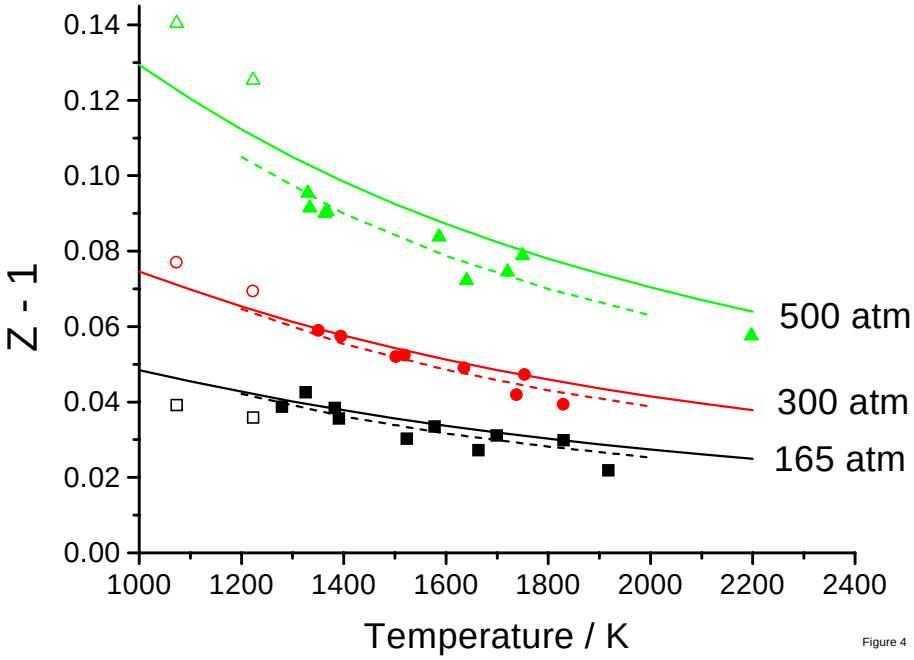

Fig. 4. Argon Compressibility Measurements: Calculated Pressure Analysis. Triangles, 500 atm data; circles, 300 atm data; squares, 165 atm data; dashes lines, least squares fit to data; solid lines, Stewart-Jacobsen (1989); hollow symbols, LeCocq (1960).

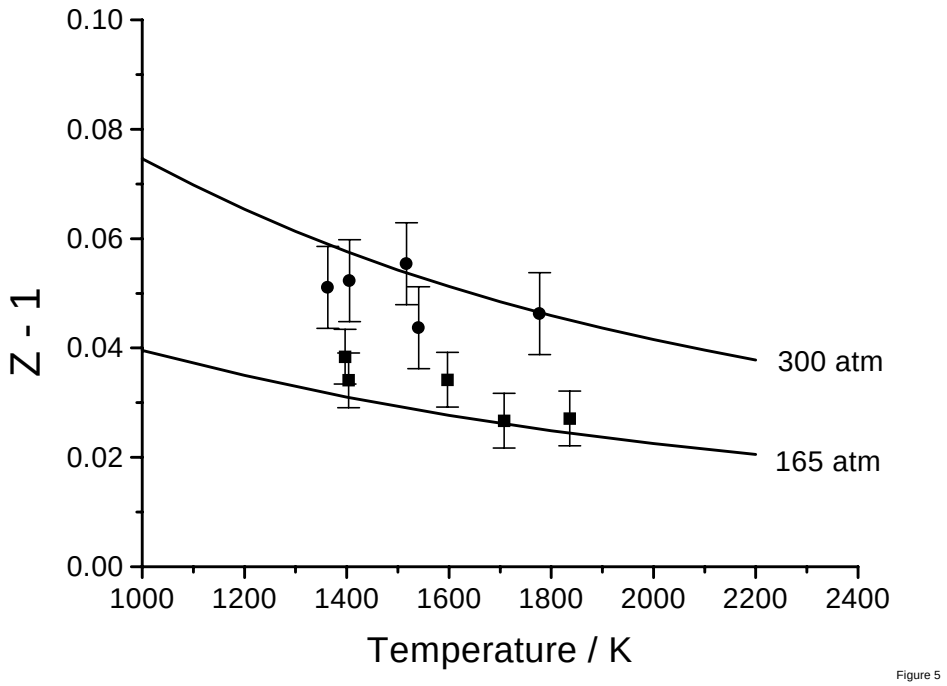

Fig. 5. Argon Compressibility Measurements: Measured Pressure Analysis. Solid lines, Stewart-Jacobsen (1989); circles, 300 atm data; squares, 165 atm data.

Over the temperature range of 1280 to 1830 K, values of B = 25.1 $cm^3 mol^{-1}$ at 165 atm, 21.2 at 300 atm, and 20.7 at 500 atm were recovered. (A single 500 atm data point taken at 2200 K is also in excellent agreement with this expression.) The fits to the data are in agreement with the available LeCocq data at 1083 and 1223 K, and differ from the extrapolation of the Stewart-Jacobsen EOS only at 500 atm. The data differs less from the Stewart-Jacobsen EOS than does the LeCocq data.

Fig. 5 shows a subset of the same data analyzed using measured pressures where reliable single PZT measurements were available. In Fig. 5 the 165 atm data is tightly clustered and has a scatter of approximately ±0.5 %. The data averages about 0.25% higher in density than the Stewart-Jacobsen values, well within the uncertainty of the present method. The 300 atm data has a slightly larger scatter ±0.75 %. The data averages about 0.5% lower than the Stewart-Jacobsen values, again within the uncertainty of the present method. The small systematic difference between the results of Figs. 5 and 4 is a result solely of the difference in the reflected shock pressure determination, and is related to uncertainties in the single pressure transducer calibration. Improvements in the pressure measurement should be possible using multiple PZT and improved thermal protection. These improvements should reduce the scatter of the data in the measured pressure analysis, bringing it in line with that of the calculated pressure analysis.

4. SUMMARY

We have measured the state variables pressure, density and temperature for argon at 165, 300 and 500 atm in the temperature interval 1280 to 1830 K using a new shock tube method. These P-ρ-T measurements are in agreement with the static cell data of LeCocq,

and validate the use of the Stewart-Jacobsen EOS formulation over a wider range of conditions than was originally published. However, some differences in the compressibility from those predicted by Stewart-Jacobsen were seen at 500 atm.

Accurate EOS measurements continue to be needed for high pressure combustion work. This is particularly so for shock tube facilities where test gas state variables are determined from thermodynamic relationships. The new technique described here, based on transient shock-wave heating and IR emission, should offer a useful new strategy for measuring or validating real gas EOS at combustion temperatures for gases other than argon.

ACKNOWLEDGEMENTS

This work was funded by the Office of Naval Research, with Dr. Richard Miller as contract monitor.

REFERENCES

1. R. G. Schmitt, P. B. Butler, Combust. Sci. and Tech. 106, 167-191 (1995).

2. D. L. Buckwalter, C. Knowlen, and A. P. Bruckner, AIAA-96-2945, 32nd AIAA Joint Propulsion Conference, Lake Buena Vista (1996).

3. C. F. Melius, N. E. Bergan, and J. E. Shepherd, 23rd Symposium (International) on Combustion, Combustion Institute, Pittsburgh, p. 217 (1990).

4. R. B. Stewart and R. T. Jacobsen, J. Phys. Chem. Ref. Data 18, 639 (1989).

5. Rabinovich, V. A.; Vasserman, A. A.; Nedostup, V. I.; and Veksler, L. S.; Thermophysical Properties of Ne, Ar, Kr and Xe, Hemisphere, Washington (1988).

6. A. LeCocq, J. Rech. C.N.R.S. 50, 55 (1960).

7. S. L. Robertson, S. E. Babb Jr., and G. J. Scott, J. Chem. Phys. 50, 2160 (1969).

8. A. Michels, J. M. Levelt, and W. De Graaff, Physica 24, 659 (1958).

9. D. F. Davidson and R. K. Hanson, Israeli J. Chem. 36, 321 (1997).

10. E. W. Lemmon, R. T. Jacobsen, S. G. Penoncello, and S. W. Beyerlein, ALLPROPS: Version 4.1, Report # 95-1, Center for Applied Thermodynamic Studies, University of Idaho (1995).

11. P. L. Vargese and R.K. Hanson, J. Quant. Spectrosc. Radiat. Transfer 26, 339 (1981).